THE 4TH INTERNATIONAL CONFERENCE ON ALUMINUM ALLOYS

PHYSICAL PROCESSES OF CRACK CLOSURE OBSERVED IN THE INTERIOR OF AN AL-LI 2090 COMPACT TENSION SAMPLE

A. Guvenilir[1], S.R. Stock[1], M.D. Barker[2] and R.A. Betz[2]
[1]Georgia Institute of Technology, School of Materials Science and Engineering, Atlanta, GA 30332-0245, USA
[2]Lockheed Missiles & Space Co., O/9369 B/203, 3251 Hanover St., Palo Alto, CA 94304-1191, USA

Abstract

Understanding the physical basis of macroscopic, indirect measurements interpreted as fatigue crack closure requires nondestructive, microscopic quantification of the crack face separations as a function of applied load. Nondestructive sectioning by high resolution computed tomography allows this to be done, and this paper reports physical crack openings measured with x-ray tomography at several loads in a compact tension sample of Al-Li 2090. These measurements, done noninvasively within the interior of the sample, are discussed in terms of crack face geometry and are compared to earlier in situ x-ray computed tomography results from loaded notched tensile samples.

Introduction

If, during unloading, the opposite faces of a fatigue crack come into contact before the minimum load is reached, crack closure is said to be occurring. This phenomenon can cause redistribution of near-crack-tip stress and strain fields, thereby lowering the effective stress intensity range and reducing fatigue crack growth rates. Oxide-induced closure [1], plasticity-induced closure [2] and roughness-induced closure [3] are mechanisms to which reduced fatigue crack growth rates have been attributed. In materials exhibiting planar glide and having macroscopically rough fracture surfaces, which includes the Al-Li system, it has been suggested that roughness-induced closure is particularly important [4]. The processes operating during crack closure can only be inferred from macroscopic load-displacement behavior or from fractography of failed or sacrificed samples, but observation of samples during in situ loading in a scanning electron microscope (SEM) has illustrated the physical processes at the samples' surfaces [5].

Recent work combining in situ loading and very high resolution x-ray computed tomography has shown that cracks can be imaged nondestructively in the interior of samples and that spatial resolution and contrast suffice for quantification of the variation of crack opening with position and with applied load [6]. Computed

tomography combines absorption profiles (i.e., radiographs) from many different viewing directions into a cross-sectional map of x-ray absorptivity within the specimen, and spatial resolution approaching 1 μm can be obtained in samples with cross-sectional dimensions as large as 2 mm [7]. Excellent agreement between tomographic sections and polished sections has also been shown [8]. The reconstructions in computed tomography provide significant advantages over radiography: overlapping images in projections are eliminated and crack visibility is much greater (which is a particular advantage for highly non-planar cracks such as those encountered in Al-Li 2090).

The earlier work with very high resolution x-ray computed tomography, however, was done on 2 mm diameter notched tensile samples of Al-Li 2090, mainly because this geometry is ideal for tomography [6]. A more conventional fatigue sample geometry is, however, required to link tomography measurements of crack closure to the body of prior work on crack closure. Such a link would be provided by computed tomography during in situ loading of compact tension samples, and this work reports the first such experiments done with microscopic spatial resolution.

Experimental Procedures

The compact tension sample CT-2 was of Al-Li 2090 T8E41 (from the same plate studied earlier [6,9]), was in the L-T orientation, was scaled in accordance with ASTM E-399-83 (31.8 mm length, 30.5 mm width and 2.0 mm thickness) and was machined from the central portion of the plate. Each side of the sample was grooved about 0.13 mm in order to restrict crack growth to a plane perpendicular to the load axis. Using an R-ratio of 0.1 and a 5 Hz haversine waveform, twelve samples were fatigued under ambient conditions using load control and a standard servohydraulic machine. Changes in compliance, monitored by differences in clip gage output, were used to estimate crack length and growth rates because locating the crack in the grooves with a microscope was problematic.

Fatigue crack growth rates were essentially identical with those reported by others [9] on full-sized compact tension samples, and, for brevity, only particulars for sample CT-2 will be reported here. After pre-cracking, the crack length was 5.6 mm, and at the end of the test, after 651,080 cycles, the crack tip was about 15.2 mm from the load line (i.e., with W = 25.4 mm, the remaining uncracked ligament was about 10.2 mm). The corresponding stress intensity ranges were 15 and 19 MPa$\sqrt{m}$, respectively. The reader should note that P_{max} was initially 106 kg and it was decreased periodically to prevent unstable crack growth.

High resolution x-ray computed tomography of sample CT-2 was performed under load using a high resolution digital radiography system at Lockheed [10]. A 2048 x 2048 x 12 bit fiber-coupled camera system was used with a 10 μm focal spot of a Kevex microfocus source operated at 160 kV and 0.06 mA and with a geometrical magnification of 1.8. Images were acquired at 359 angles (the rotation axis was parallel to the stress axis), each radiograph was recorded with 10 sec exposure and the volume

containing the crack was reconstructed with isotropic 20 μm voxels (i.e., volume elements) using the Feldkamp cone beam reconstruction algorithm [11]. During data collection, the sample was mounted in a portable, pneumatically-driven load frame developed for use in x-ray computed tomography [12]. Data was collected at five applied loads: 42, 35, 28, 21 and 8 kg. The maximum load was that the sample experienced during the final increment of crack growth.

Results and Discussion

The three-dimensional volume of material containing the crack can be numerically sectioned along any arbitrary plane. In the case of sample CT-2, these are the planes which both contain the stress axis and are perpendicular to the sample face (Figure 1); in other words, the cuts span the sample thickness from one side-groove to the other. Figure 1 shows every tenth cut, i.e., the 20 μm thick cuts of material are spaced by 200 μm, at the highest load. The numbers in the lower left of each cut give the cut's distance in mm from the notch tip. Darker pixels correspond to voxels with lower absorption, the tips of the two side-grooves (1.75 mm apart) are visible at the left and right center of each image and the stress axis is vertical.

The series of cuts reveals that volumes of asperity-dominated crack geometry alternate with relatively planar sections of the crack. Considerable crack branching is visible throughout. The multiple asperities in the material nearest the notch give way to a single large asperity (seen near the left side-groove in cuts 0.3 through 1.1) on one side of a relatively flat crack. The gentle waviness of the crack continues between 1.3 and 3.1 mm, with the crack inclined at a slight angle to the surface in cuts between 1.3 to 1.9 mm, a transition region where the crack bows concave up and the crack running directly across the sample between cuts 2.3 and 3.1 mm from the notch.

Multiple asperities dominate the crack geometry from 3.3 to 6.1 mm. After this the crack becomes relatively flat until 8.1 mm where the asperities appear to become important once again. The contrast from the crack begins to disappear beyond 8.3 mm for cuts at 8 kg load, but at 42 kg load the crack is visible across the entire cross section until about 8.6 mm. Some discontinuous-appearing sections of the crack are seen until about 9.6 mm, which is about the maximum extent of the crack in carefully aligned radiographs, but the contrast of the crack differs little from the noise in the image surrounding it. The compliance measurements indicate that the crack extended about 9.7 mm from the notch, which is in good agreement with the tomographic results. The sample is still intact, so that no further comparisons can be made between the actual crack surface and the tomography results.

Crack opening was measured numerically in several steps. First the average value of the linear attenuation coefficient μ_{avg} of the voxels of uncracked material was determined away from the crack, and any voxels with $\mu < 0.9\mu_{avg}$ were identified as potentially being partially or totally occupied by a crack. The approximate position of the crack was marked manually, and the value of each voxel above

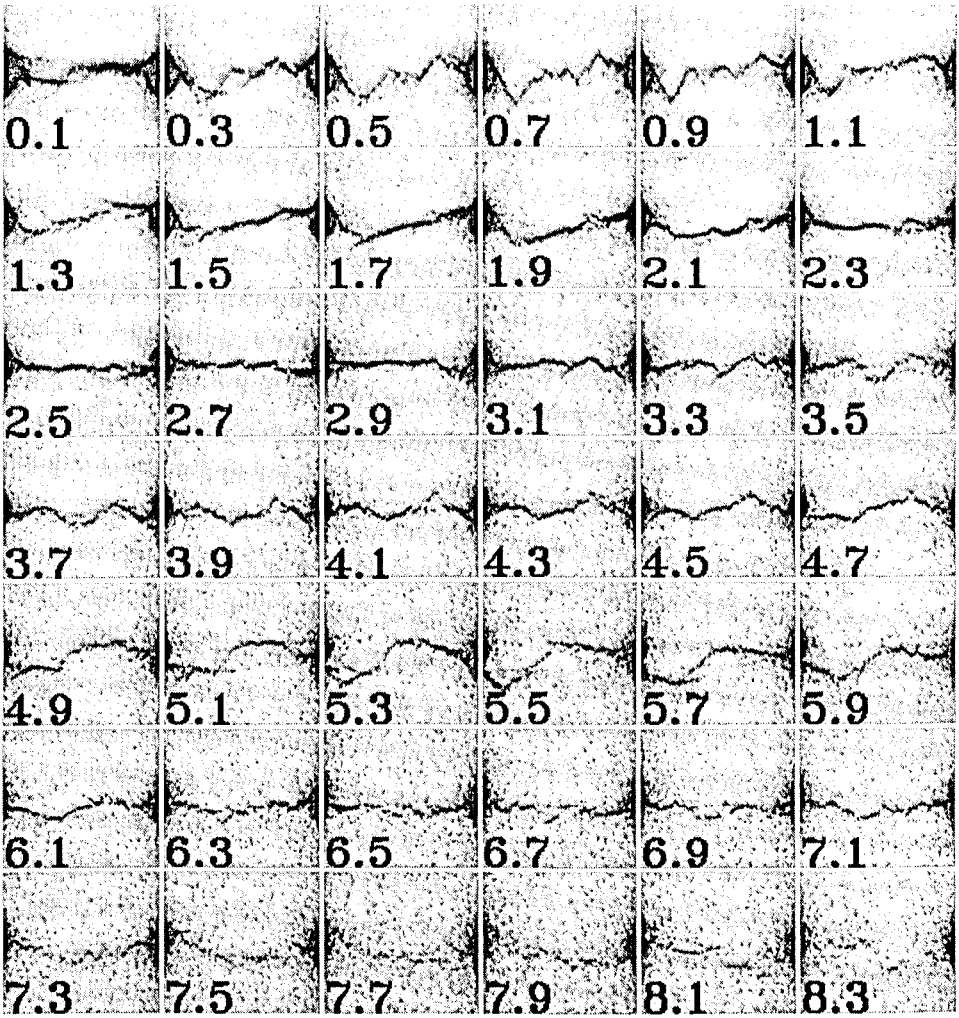

Figure 1. Series of reconstructed sections parallel to the notch tip and showing the crack morphology in sample CT-2. Lower absorption pixels are darker, and the numbers indicate the distance between the cut and the tip of the notch (in mm). The two side-grooves appear on the left and rights sides of each cut, and their separation is 1.75 mm.

and below the approximate center of the crack was checked until a value of $\mu > 0.9\ \mu_{avg}$ was encountered. The partial volumes of crack in the voxels between the two limits were then summed to give the total crack opening.

Figure 2 shows two pairs of cuts at the maximum and minimum loads (42 and 8 kg, respectively), and this clearly shows the amount and location of the physical crack closure. The location of the top and bottom pairs of cuts are 2.96 mm and 5.12 mm, respectively, from the end of the notch, and these are used to illustrate measurements for different crack morphologies. The total crack opening at each position is shown in the plot below each pair of cuts; the uppermost curve gives the opening at the higher load. Across the two thin volumes of material, there is considerable variation in crack opening and in the amount the opening changes (which gives the amount by which the two crack faces have moved together). In these two cuts the flatter areas of the crack tend to be more open, and subtle differences with position in a single cut are seen in the amount of crack closure. At other locations which are not shown here, however, large differences in crack closure are seen in adjacent areas of the crack. Openings from crack branches away from the main crack are not included here. When crack branching is seen, the crack openings of the branches are recorded separately for further analysis.

Conclusions

Results of high resolution x-ray computed tomography obtained under load were presented for a cracked compact tension sample of Al-Li 2090. Crack morphology was determined noninvasively, and two examples of the measurement of crack opening were shown as a function both of position and of applied load.

Acknowledgements

This research was supported by ONR grants N00014-89-J-1708 and N00014-94-1-0306. We thank Mr. R.C. Brown, Mechanical Properties Research Laboratory at Georgia Tech, for his assistance with mechanical testing issues. We are very grateful to Dr. T. M. Breunig, presently at Sandia National Laboratory-Livermore, who grew the fatigue crack in sample CT-2 and who helped nucleate this activity in crack closure.

References

1. R.H. Christensen, Appl. Mat. Res., Oct. 1963, 207.

2. W. Elber, in Damage Tolerance in Aircraft Structures, ASTM STP 486, (ASTM, Philadelphia, 1971) 230.

3. S. Suresh and R.O. Ritchie, Met. Trans. 13A, (1982), 1627.

4. R.O. Ritchie, in Fatigue Thresholds, ed. J. Backland, A. Blom and C.J. Beevers, (Engineering Advisory Services, Ltd., Warley, UK, 1981) 503.

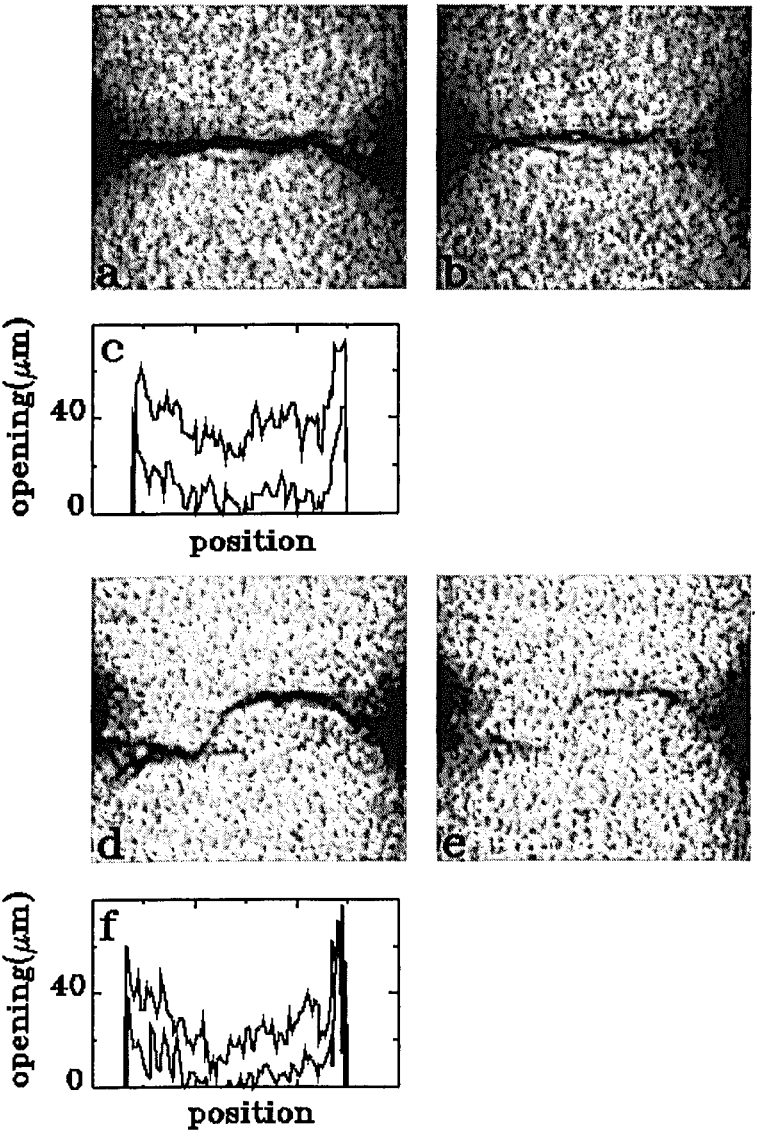

Figure 2. Cuts and measured crack openings. In the images the darker pixels show lower x-ray attenuation, the stress axis is vertical and the ends of the side-grooves, visible at the left and right center of each image, are 1.75 mm apart. a. and b. are cuts 2.96 mm from the end of the notch under 42 kg and 8 kg load, respectively. d. and e. are cuts 5.12 mm from the notch under 42 kg and 8 kg load, respectively. c. and f. show crack opening across each cut 2.96 mm and 5.12 mm from the notch, respectively; the upper curve in each corresponds to the higher load.

5. J. Lankford, D. Davidson and K.S. Chan, Met. Trans. 15A, (1984), 1579.

6. T.M. Breunig, S.R. Stock, S.D. Antolovich, J.H. Kinney, W.N. Massey and M.C. Nichols, in Fracture Mechanics: Twenty-second Symposium (Volume I), ASTM STP 1131, (ASTM, Philadelphia, 1992) 749.

7. J.H. Kinney, Q.C. Johnson, U. Bonse, M.C. Nichols, R. Nusshardt, R. Pahl and J.M. Brase, MRS Bull. XIII, (1988) 13.

8. J.H. Kinney and M.C. Nichols, Annu. Rev. Mater. Sci. 22, (1992) 121.

9. G.R. Yoder, P.S. Pao, M.A. Imam and L.A. Cooley, in Proceedings of the Fifth International Aluminum-Lithium Conference, ed. T.H. Sanders, Jr. and E.A. Starke, Jr., (Materials and Component Engineering Publications, Ltd, Birmingham, UK, 1989) 1033.

10. C. Bueno, M.D, Barker, R.C. Barry, R.A. Betz and S.M. Jaffey, to appear in the proceedings of the 39th International SAMPE Symposium, April 11-14, 1994, Anaheim, CA.

11. L. Feldkamp, L.C. Davis and J.W. Kress, J. Opt. Soc. Am. 1, (1984) 612.

12. T.M. Breunig, S.R. Stock and R.C. Brown, Mat. Eval. 51, (1993) 596.